

Further Study on the Micellization of a Symmetric Amphiphile Using the Monte Carlo Technique

Hussein Gharibi,[1,2] **Reza Behjatmanesh-Ardakani,***[1,3] **Seyed Majid Hashemianzadeh,**[1] **Beheshteh Sohrabi,**[1] **and Soheila Javadian**[1]

[1]Department of Chemistry, Tarbiat Modarres University, P. O. Box 14155-4838, Tehran, Iran

[2]Iranian Information and Documentation Center (IRANDOC), P. O. Box 13185-1371, Tehran, Iran

[3]Department of Chemistry, School of Science, Payame-Noor University, Ardakan, Yazd, Iran

Received November 16, 2005; E-mail: Reza_b_m_a@yahoo.com

We use a modified version of Larson's model to investigate the behaviors of amphiphile molecules in different states of interaction parameters. The regular excluded volume and periodic boundary conditions are used to mimic a box of simulation as a bulk of solution. Several thermodynamic parameters are studied by lattice Monte Carlo simulation, including polydispersity, premicellar phenomena, critical micelle concentration, aggregation number, and cluster shape. For higher interaction parameters aggregation starts at lower concentration, i.e. critical micelle concentration is reduced. Behaviors are linear. With linearizing matrix of gyration, it is shown that at higher interactions micelles tends to reduce their contacts with water, so they take the shape of a sphere. In all of the cases, cluster size distribution has only one peak. Polydispersity behavior indicates that it is possible to determine critical micelle concentration from the polydispersity curve. Configurational bias and reptation moves are used with equal probability to relax the amphiphilic systems. To investigate meta-stability in the thermodynamic parameters two different initial conditions are used.

Amphiphilic systems have been investigated in many fields of research by various techniques. These systems have been examined experimentally using approaches such as surface tension measurements,[1,2] spectroscopy,[3,4] potentiometry,[5,6] and chromatography.[7] In addition, theoretical studies have been carried out aimed at explaining and predicting the behavior of these complex systems.[8,9] A key tool in the theoretical modeling of amphiphilic systems has been molecular simulation. Various simulation strategies have been developed to cope with the enormous range of time scales of the motions within these systems. Four simulation techniques that have proved popular are Monte Carlo, molecular dynamics, Brownian dynamics, and time-dependent Ginzburg–Landau equations.[10]

Monte Carlo and molecular dynamics techniques have been implemented as lattice[11] and off-lattice[12–14] models. Lattice models are simpler and more efficient than off-lattice models because they do not include atomistic details of molecules. Instead of such details, the "molecules" on the lattice are modeled as strings of beads that interact via predefined interaction parameters. In the present study, we investigated the role of the interaction parameter on micellar systems.

In this work, using a lattice model, investigation of the thermodynamics of a self-assembling process is approached. So, we have considered surfactant molecules as connected beads with two different characteristics. Beads that are similar to water have hydrophilic properties and are named as heads (H), and beads that behave like oil are hydrophobic and named as tails (T). In this study, we have considered a chain containing 4H and 4T beads (H_4T_4) as a surfactant molecule. It is shown how a model containing only repulsive interactions can predict the effects of temperature variations on the thermodynamic behaviors of aggregates.

Theoretical

Model. A number of models have been used to simulate amphiphiles in lattice models. One family of models that has been widely used consists of a simple square or cubic lattice with only the nearest neighbor interactions. The coordination numbers of these lattices for two and three dimensions are 4 and 6, respectively.[15–28]

Models based on non-cubic lattices have also been developed. For example, Nelson and co-workers used two-dimensional triangular lattices and three-dimensional face-centered cubic lattices,[29,30] and Haan and Pratt used a diamond lattice to study micellar clusters.[31]

Variation of the lattice coordination number changes the thermodynamic parameters of micellization, making it impossible to directly compare the results of different models for the same amphiphile.

In addition to the above variables, the interaction parameters depend upon the assumptions used in the model. For example, the interaction parameters in some models are set by assuming that repulsive forces dominate, whereas other models assume that attractive forces dominate. Care and co-workers[19,20,26] considered repulsive interactions between tail–solvent and head–head, but attractive inteactions for head–solvent beads:

$$\frac{U}{kT} = \beta\left(n_{TS} + \gamma n_{HS} + \eta n_{HH} + \sum_i \varepsilon_c^i\right), \quad (1)$$

where n_{HH}, n_{TS}, and n_{HS} are the numbers of head–head, tail–

Published on the web September 5, 2006; doi:10.1246/bcsj.79.1355

solvent, and head–solvent interactions, β is the ratio of tail–solvent energy to kT, γ is the ratio of the head–solvent to tail–solvent energy, η is the ratio of the head–head energy to the tail–solvent energy, and ε_c^i is the chain conformational energy normalized by the tail–solvent energy. The parameter β is chosen to be positive and the parameter γ is chosen to be negative. For simplicity, in Care's model the chains are supposed fully flexible (i.e. $\varepsilon_c^i = 0$) and the head–head interactions are neglected (i.e. $\eta = 0$).

On the other hand, some authors have utilized Larson's model[32–36] in which a lattice site is either oil-like (L) or water-like (H). In this model, it is shown that in any transition, the net change in the number of lyophilic–lyophilic (LL) interactions equals the net change in the number of hydrophilic–hydrophilic (HH) interactions, which in turn equals $-1/2$ times the net change in the number of lyophilic–hydrophilic (LH) interactions. It follows that the net energy associated with any fluctuation is a multiple of $W = E_{LL} - \frac{1}{2}E_{LL} - \frac{1}{2}E_{HH}$, where E_{LH}, E_{LL}, and E_{HH} are the energies of LH, LL, and HH interactions, respectively. The dimensionless reciprocal temperature, $w = \beta W$, and the overall composition are therefore the only intensive variables of Larson's lattice model.

In the present work, our model is a modified version of Larson's model with a reducing cut-off range of interactions from $z = 26$ to $z = 6$, where z is the coordination number. To prove this equivalence one can suppose total contact for a site (n_c) in Larson's model as

$$n\_c = n\_LH + n\_HH + n\_LL, \tag{2}$$

with assuming $E_{LL} = E_{HH}$, the following equation can be written for total energy of a configuration:

$$E = n\_LH \times E_{LH} + (n\_HH + n\_LL) \times E_{LL}, \tag{3}$$

with some modification the equation changes to

$$\begin{aligned} E &= n\_LH \times E_{LH} + (n\_c - n\_LH)E_{LL} \\ &= n\_LH(E_{LH} - E_{LL}) + n\_c \times E_{LL}. \end{aligned} \tag{4}$$

Since $n\_c \times E_{LL}$ and $E_{LH} - E_{LL}$ are constant, the energy difference, i.e. the acceptance probability, for both models is the same.

The model used here contains the repulsions between unlike sites: tails with heads (T–H) and tails with water (T–W). In other words, we did not use attractive interactions such as T–T and H–H that have been used in Care or Larson's model.

Although most of these works were carried out in a canonical ensemble (constant volume, temperature, and number of components), some other useful methodologies have been used to study micellization and phase transitions. Panagiotopoulos and co-workers have used the Gibbs ensemble[37] and the grand canonical ensemble[38–40] to study amphiphilic and polymeric systems.

An important consideration in the implementation of all of the above models and approaches is that the simulated system must be relaxed to achieve a true ensemble averaging for a thermodynamic function. Thus, program code that rapidly brings the system to the relaxed state is desirable, and this need has prompted the introduction of different types of lattice moves. Examples of local motions used in lattice simulations are endflip motion, crank-shaft motion, kinkjump motion,[41,42] reptation move,[43,44] general reptation move,[45,46] and configurational bias Monte Carlo move.[47] The general reptation method and configurational bias Monte Carlo method have been shown to be the most efficient approaches.[45,47] Our simulations are based on the standard Metropolis algorithm[48] in which we have used the probability of $P = \mathrm{Min}(1, \exp(-\beta\Delta E))$ for reptation move and probability $P = \mathrm{Min}(1, \frac{W(n)}{W(o)})$ for configurational bias Monte Carlo move. ΔE is the difference of the total energy between new trial and old configurations, β is $1/(k_B T)$ and P is the probability by which new trial configuration is chosen. W is the Rosenbluth weight, which is defined as

$$W(n) = \prod_{i=1}^{l} w_i(n) \quad \text{and} \quad w_i(n) = \sum_{j=1}^{k} \exp(-\beta u_i(j)), \tag{5}$$

where $u_i(j)$ includes all interactions of segment i with other molecules in the system and with segments 1 through $i-1$ of the same molecule. It does not include interactions with segments $i+1$ to l.

In the present work, we focus only on the main characteristic of amphiphile molecules, which is the repulsion between unlike sites (tail–water or tail–head). So, we used the following model:

$$\frac{E}{k_B T} = \frac{\varepsilon}{k_B T}(n_{T,w} + n_{T,H}), \tag{6}$$

where E is the total energy of the configuration, k_B is the Boltzmann constant, $n_{T,w}$ and $n_{T,H}$ are the number of tail–water and tail–head contacts, respectively, which are in the nearest neighbors of each other. In this paper, we change the value of $\varepsilon/k_B T$ (interaction parameter) and study the effects of the interaction parameter on the aggregation process. Because increasing or decreasing the interaction parameter affects the value of hydrophobicity of tail sites, it is possible to investigate the role of hydrophobicity on the thermodynamics of aggregation.

Only nearest neighbors ($z = 6$) are considered and a lattice with dimensions of $50 \times 50 \times 50$ to reduce size effects in the simulations. Since the reptation move is non-ergodic,[49] reptation in conjunction with configurational bias Monte Carlo move is used with equal probabilities. To study the role of hydrophobicity, different values of interaction parameters are used ranging from 0.7 to 0.8.

Definition of Parameters. Two amphiphile chains are considered to be in the same cluster if any tail site of the first molecule is a nearest neighbor of any tail site of the second molecule.

This definition of an aggregate has been used extensively.[13,38,50,51] Amphiphiles that do not form part of an aggregate are monomers. During the simulations, the monomer mole fraction (x_1), cluster mole fraction with aggregation number n (x_n), and the distribution of monomers in different clusters (nx_n) are calculated with the following definitions:

$$x_1 = \frac{\text{number of free amphiphiles}}{\text{total number of molecules in lattice}}, \tag{7}$$

$$x_n = \frac{\text{number of aggregates of } n \text{ amphiphiles}}{\text{total number of molecules in lattice}}, \tag{8}$$

$$x_a = \frac{\text{total number of amphiphile molecules}}{\text{total number of molecules in lattice}}. \tag{9}$$

It is clear that the following equation is obeyed:

$$x_a = \sum_{n=1}^{\infty} nx_n. \tag{10}$$

To study shape behaviors, the matrix of the radii of gyration ($R^2_{i,j}$) is calculated for clusters with aggregation numbers greater or equal to 10. This matrix is defined as

$$R^2_{i,j} = \frac{1}{S}\sum_{k=1}^{s}(r_{i,k} - r_{i,\mathrm{cm}})(r_{j,k} - r_{j,\mathrm{cm}}), \tag{11}$$

where $r_{i,k}$ $(1 \le i \le 3)$ represents the lattice location for the kth site in the aggregate, S is the total number of sites occupied by the aggregate, and $r_{i,\mathrm{cm}}$ and $r_{j,\mathrm{cm}}$ are the centers of mass in directions i and j, which are given by $r_{i,\mathrm{cm}} = \frac{1}{S}\sum_{k=1}^{S} r_{i,k}$ and $r_{j,\mathrm{cm}} = \frac{1}{S}\sum_{k=1}^{S} r_{j,k}$, respectively. The three principal moments of inertia, I_1, I_2, and I_3 are obtained from the eigenvalues of this matrix. The characteristic lengths are defined as $l_i = (I_i)^{1/2}$. For spherical aggregates, $l_1/l_3 = l_2/l_3 = 1$; and for cylindrical micelles, $l_1/l_3 \gg 1$ and $l_2/l_3 = 1$.

Three kinds of aggregation number can be defined: (a) $N_{\max}$ (maximum of the monomer distribution curve in which nx_n is plotted against n), (b) N_n (number-averaged aggregation number), and (c) N_w (weight-averaged aggregation number). N_n and N_w are defined as follows:

$$N_n = \frac{\sum_{n=2}^{n_{\max}} nx_n}{\sum_{n=2}^{n_{\max}} x_n}, \tag{12}$$

and

$$N_w = \frac{\sum_{n=2}^{n_{\max}} n^2x_n}{\sum_{n=2}^{n_{\max}} nx_n}, \tag{13}$$

where $n_{\max}$ is the maximum aggregation number in all of the snapshots considered in the ensemble averaging. The monomeric form is not considered as an aggregate, and hence is not included in the above equations. The polydispersity is defined as the ratio of N_w to N_n. For clusters of size $n \ge 10$ in the monomer distribution curve, the value of nx_n is averaged over aggregates of size $n \pm 2$ in order to reduce statistical fluctuations, and thus to obtain a smooth distribution. Aggregates comprising less than 10 monomers are often referred to as premicelles.[52]

Another parameter that should be defined is the critical micelle concentration (CMC). Various definitions for the CMC have been used in the literature.[19–26,53–59] We use Israelachvili's definition,[54] which defines the CMC as the concentration at which $x_1 = \sum_{n=2}^{\infty} nx_n$.

Results and Discussion

Reliability on Simulation Results. Bernardes et al.[25] have reported that simulation data can be deemed reliable only if I) the data do not derive from a meta-stable state, II) the system is fully relaxed, III) there are no finite size effects, and IV) there is no correlation between snapshots. So, the results must be checked on the basis of the above cases. To investigate meta-stability and relaxation we have used two different initial configurations (one highly random and the other highly ordered).[25]

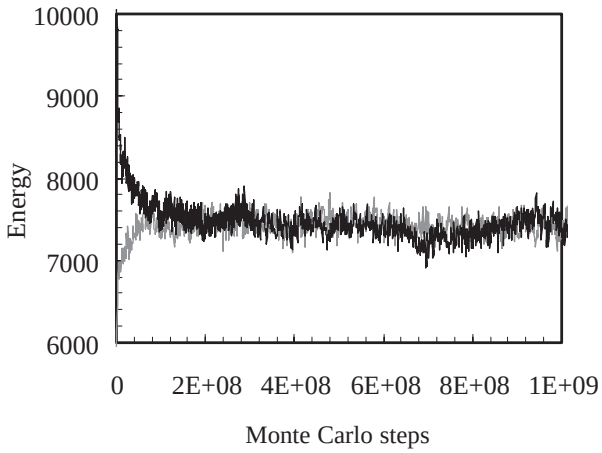

Fig. 1. Convergence of two different configurations (highly random and highly ordered).

The random initial configuration can be constructed as follows. At first, the total sites of the lattice are filled by water. Then, a site in the lattice is chosen at random and one surfactant molecule is grown there. The above process is repeated until all of the surfactant molecules are located on the lattice. For the ordered initial configuration, contrary to the random state, at first the lattice is filled by surfactant molecules in an aggregate shape. Then, all of the unoccupied sites are filled by water molecules. Almost all of the lattice simulations use the two different initial configurations described above. Thermodynamic properties of these two different initial configurations converge if there is not any meta-stability.

Figure 1 shows the relaxation behavior of our system during two relaxation procedures: (1) cooling of a random initial configuration to $\varepsilon/k_BT = 0.8$, and (2) warming of a highly ordered initial configuration to $\varepsilon/k_BT = 0.8$. For both procedures, the system relaxed to the same fluctuation range. This convergence is achieved in all cases due to the condition of microscopic Monte Carlo moves. On the other hand, true ensemble averaging needs to avoid any correlation between snapshots taken for averaging. This condition is investigated by calculation auto-correlation function. Figure 2 illustrates an energy auto-correlation function for a simulation with the interaction parameter equal to 0.8. The energy auto-correlation function is defined as

$$A(\tau) = \frac{\langle E(t+\tau)E(t)\rangle - \langle E(t)\rangle^2}{\langle E^2(t)\rangle - \langle E(t)\rangle^2}, \tag{14}$$

where $A(\tau)$ is the correlation between snapshots at time t and $t + \tau$. It is clear that the maximum of correlation takes place at $t = 0$ and the minimum of it is zero at snapshots that are independent of each other. $E(t)$ is the total energy of lattice at time t and $E(t + \tau)$ is the total energy for time $t + \tau$; $\langle\cdots\rangle$ refers to the averaging over snapshots. It must be noted for getting a smooth curve, very large snapshots should be taken, i.e., very long run should be done.

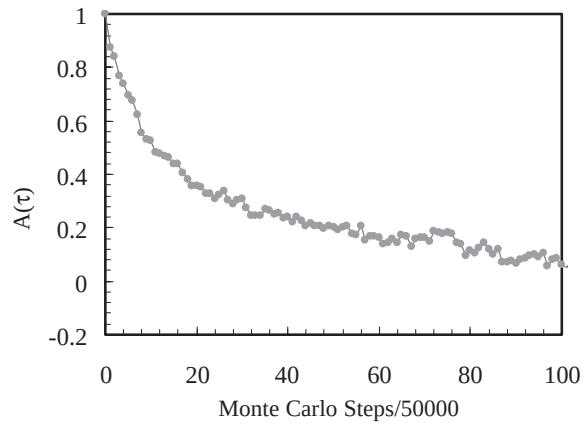

Fig. 2. Energy auto-correlation function, $A(\tau)$, versus time (Monte Carlo steps).

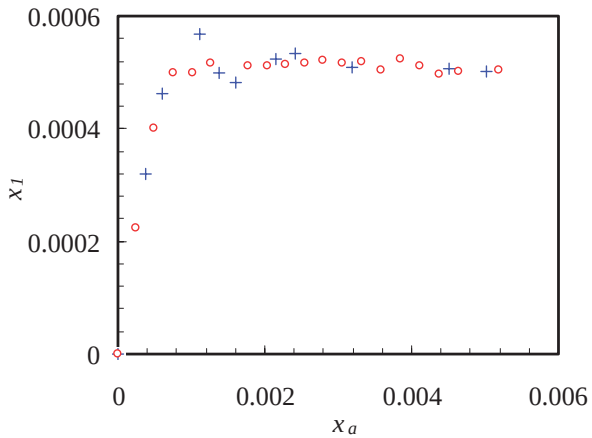

Fig. 3. Convergence of x_1 as x_a for boxes of dimensions 30 (+) and 50 (○).

As is shown in this figure, with taking 5×10^6 moves between snapshots we can avoid correlation. It must be mentioned that all of our data were checked for correlation, and finally for investigation about size-dependence of our results, we run simulation on two different boxes. Figure 3 shows how results for box sizes of 30 and 50 complement each other. So, we choose the dimension of 50 for all of our simulations.

Critical Micelle Concentration. CMC has been studied using various models and techniques.[17,19,29,60–62] Some of these studies, similar to our results, show that the CMC increases with an increase in temperature. The similarity between results indicates an important point. It represents that the fundamental part of the model in the self-assembling of surfactants is repulsion interactions, and TT or HH interactions themselves (even attractive or repulsive) are inconclusive; in other words, considering attractive parameters between like sites do not change the results.

In our simulations, the CMC increases as the value of interaction is decreased (Table 1). Fitting plots of the CMC for H_4T_4 versus ε/k_BT gives the following equation:

$$\mathrm{CMC} = -0.012\frac{\varepsilon}{k_BT} + 0.011 \quad R^2 = 0.99. \tag{15}$$

Distribution of Monomers in Clusters. The equilibrium distribution of micelle sizes is that which minimizes the free energy of the system and, by mass conservation, that condition is fulfilled by the relation $n\mu_1 = \mu_n$ (appendix A).[63] This yields the following mass-action relation:

$$x_n = \frac{(f_1 x_1)^n}{f_n} \exp\left(-n\beta\left(\frac{\mu_n^0}{n} - \mu_1^0\right)\right). \tag{16}$$

In Monte Carlo simulation, on the other hand, the proportion of monomers in clusters of size n (nx_n) can be determined. As shown in Fig. 4, nx_n as a function of n typically has a minimum and two maxima: one for the monomer and the other for the micelles.[64] It has been shown in our previous paper that even in the mixed state of amphiphile and copolymer, the cluster size distribution must have only one peak.[65] A wider distribution indicates a higher polydispersity, and the presence of a high concentration of clusters with small aggregation numbers indicates the existence of premicellar phenomena.

Table 1. CMC Values for H_4T_4 at Different Interaction Parameters (ε/k_BT)

ε/k_BT	CMC (in mole fraction)
0.72	0.0020
0.74	0.0017
0.76	0.0015
0.78	0.0013
0.8	0.0010
0.82	0.0008

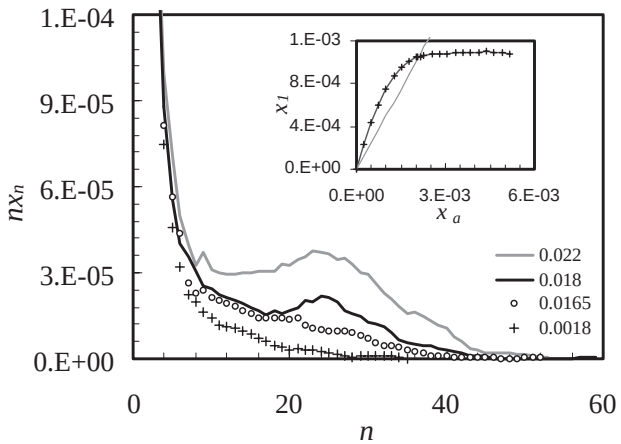

Fig. 4. Distribution of monomer in clusters at different mole fractions of H_4T_4 at $\varepsilon/k_BT = 0.72$. Inset shows a plot of x_1 against mole fraction (x_a) of surfactant.

Concentrations of Premicelle. From the distribution of monomers in clusters of different size, it is possible to determine the concentration of the small clusters that are often referred to as premicelles. Comparison of this distribution at different interactions, shown in Fig. 5, reveals that the concentrations of premicelles decrease with an increase in interaction parameter.

Figure 6 shows the dependence of the premicellar value on the mole fraction of amphiphile at various interactions. In this figure, only the cluster due to the minimum in the graph of the distribution of monomer in clusters is considered as a premicelle.

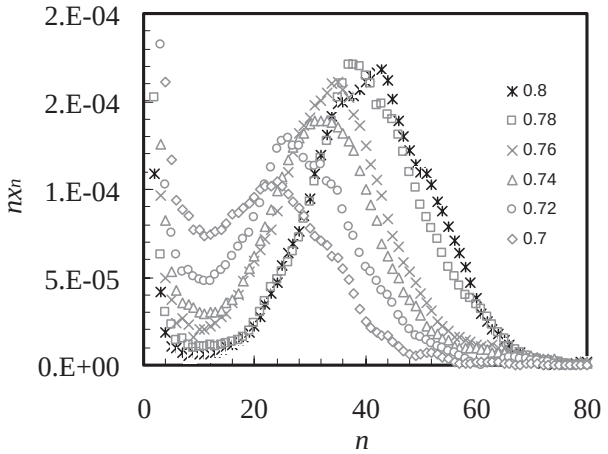

Fig. 5. Role of interaction on nx_n of premicelles. nx_n is the monomer mole fraction in a cluster containing n surfactants.

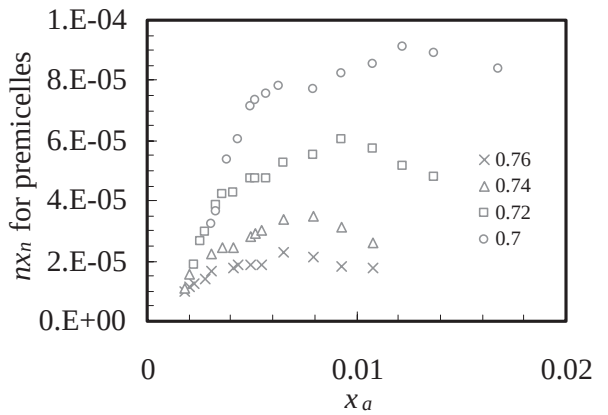

Fig. 6. Dependence of premicellar values on mole fraction of amphiphiles at various interaction parameters.

Polydispersity. Polydispersity (I_P) is the ratio of the weight-averaged aggregation number to the number-averaged aggregation number. In normal cases, it is expected that as the surfactant concentration is increased beyond the CMC, the polydispersity should decrease because introducing further surfactant molecules leads to the growth of smaller clusters, and thus the distribution of cluster aggregation numbers would become narrower. So, CMC can be defined as the amphiphile concentration at which the value of the polydispersity is greatest. Indeed, as shown in Fig. 7, this behavior is observed for all of the cases in the present work and the value of the polydispersity is greatest at the CMC. Above the CMC, increasing interactions cause a reduction in the polydispersity. Therefore, at high interactions, monomers prefer either to aggregate to form new micelles or to enter into small clusters rather than to join large aggregates. As a result, spherical aggregates rather than other shapes tend to form at high interactions.

Micellar Shapes. The micellar shapes are determined based on the three principal moments of inertia, I_1, I_2, and I_3, which correspond to the eigenvalues of the matrix of the radii of gyration.

Figure 8 shows the dependence on aggregation number of the two characteristic length ratios, l_1/l_3 and l_2/l_3, for H_4T_4 at two states of interaction. It is evident from this figure that with an increase in interactions, a transition from rod-like micelles to spherical micelles occurs at higher aggregation numbers. It is in consistant with the experimental results. At low temperature, to reduce the interfacial area (or contacts)

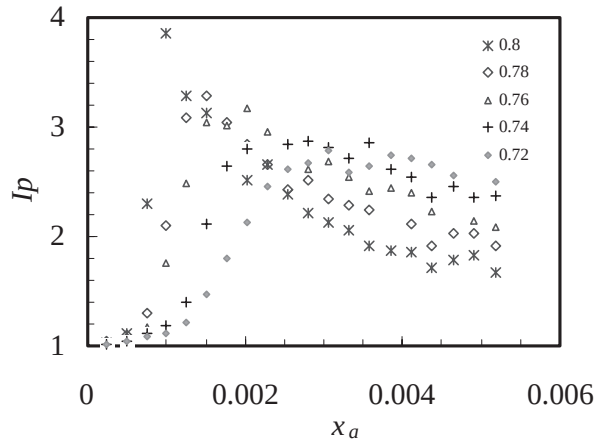

Fig. 7. Polydispersity of H_4T_4 at different interaction parameters.

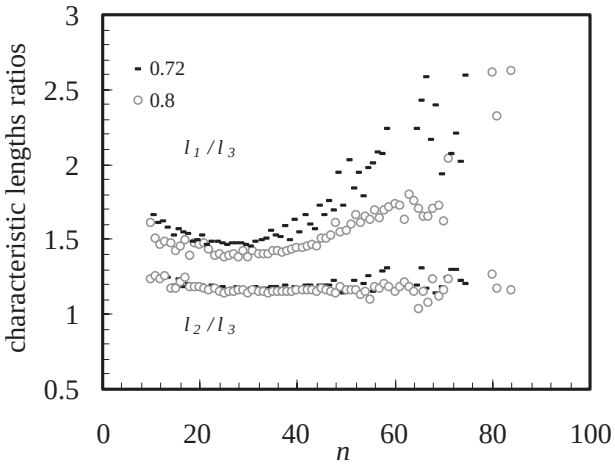

Fig. 8. l_1/l_3 and l_2/l_3 for H_4T_4 at $x_a = 0.0052$ for different interactions.

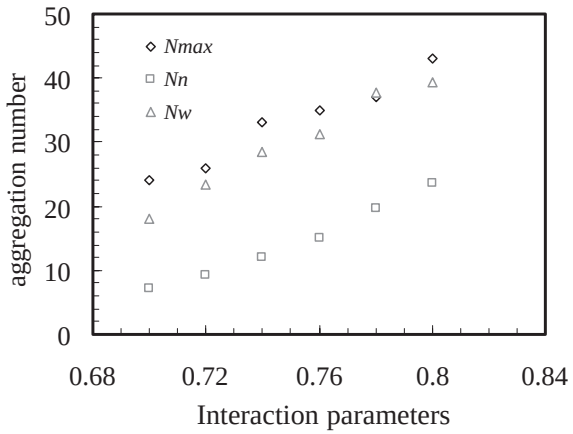

Fig. 9. Variation in aggregation number with changing interaction parameters at $x_a = 0.0052$.

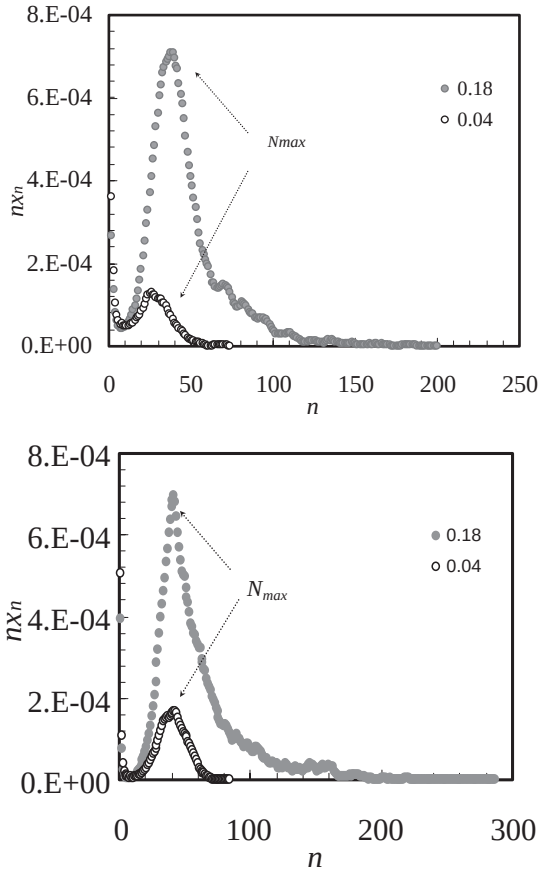

Fig. 10. a. N_{max} increases with an increase in concentration (x_a) for $\varepsilon/k_BT = 0.72$. b. N_{max} is nearly constant at two different concentrations (x_a) for $\varepsilon/k_BT = 0.8$.

the micelles tend to become spheres and to shrink.

Aggregation Number. Figure 9 shows the role of interactions on three definitions of aggregation number. For all three definitions, the aggregation number increases linearly with an increase in interaction. Fitting of a straight line to the N_w data gives the following equation:

$$N_w = 218\frac{\varepsilon}{k_BT} - 134 \quad R^2 = 0.98. \tag{17}$$

Figure 10a shows a plot of nx_n versus n at two concentrations for $\varepsilon/k_BT = 0.72$, while Figure 10b shows the same plots for the system with $\varepsilon/k_BT = 0.8$. Comparison of these figures reveals that N_{max} is less concentration-dependent for the higher interactions. Figure 11 shows the variation of N_w versus concentration at two interaction parameters. An acceptable estimate of the CMC can be determined from this curve as the intersection of a straight line fits to the curves before and after the change in slope.

Conclusion

In the present work, it is shown that the fundamental part of the potential belongs to the repulsion between tails–solvent and tails–heads. Although in most of the simulation works attractive potentials have been considered, these interactions do not play a fundamental role at least in the lattice Monte Carlo simulation of surfactants. We have also shown that an increase

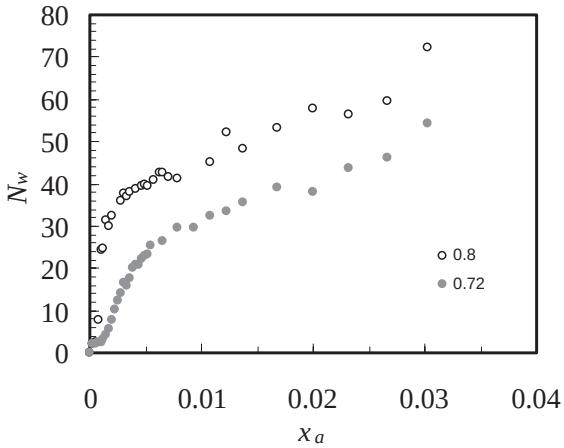

Fig. 11. Dependence of N_w on concentration for two interaction parameters.

in repulsive forces causes, similar to the CMC behavior, an increase in aggregation number and polydispersity. We obtained a linear relationship between interaction parameter and the CMC. It must be noted that at high interaction, micelles tends to be spherical rather than rod-shaped. Further studies are needed to elucidate the effect of interaction on the sphere to rod transition. Increasing interactions additionally causes a reduction in the concentration of premicelles.

We would like to thank Professor Mihaly Mezei from Mount Sinai School of Medicine in New York for his valuable discussion about configurational bias Monte Carlo move and the model through e-mail and the referees for their attention.

Appendix

In canonical ensemble, the equilibrium distribution of micelle sizes is that which minimizes the Helmholtz free energy (A) of the system. By considering the condition of

$$N = \sum_{n=1}^{\infty} nN_n, \tag{A1}$$

it is possible to minimize A by the method of undetermined multipliers.

Let λ be an undetermined multiplier. Then, we have

$$\frac{\partial A}{\partial N_n} - \lambda\frac{\partial N}{\partial N_n} = 0. \tag{A2}$$

The first term in this equation is defined as the chemical potential of aggregate n, and the second term is equal to n. Thus, we have

$$\mu_n - \lambda n = 0 \Rightarrow \mu_n = n\lambda. \tag{A3}$$

This equation is correct for all values of n. If we substitute $n = 1$, we can write

$$\mu_1 - \lambda = 0 \Rightarrow \mu_1 = \lambda. \tag{A4}$$

Then, we can substitute the new value of λ into Eq. A4:

$$\mu_n = n\lambda = n\mu_1. \tag{A5}$$

This equation is often referred to as the mass action equation for aggregates. From this equation, one can calculate the excess chemical potential.

References

1 Y. Hayami, H. Ichikawa, A. Someya, M. Aratono, K. Motomura, *Colloid Polym. Sci.* **1998**, *276*, 595.

2 C. C. Ruiz, J. Molina-Bolívar, J. Aguiar, G. MacIsaac, S. Moroze, R. Palepu, *Colloid Polym. Sci.* **2003**, *281*, 531.

3 M. Vasilescu, A. Caragheorgheopol, H. Caldararu, *Adv. Colloid Interface Sci.* **2001**, *169*, 89.

4 H. Gharibi, S. Javadian, B. Sohrabi, R. Behjatmanesh, *J. Colloid Interface Sci.* **2005**, *285*, 351.

5 H. Gharibi, B. M. Razavizadeh, M. Hashemianzadeh, *Colloids Surf., A* **2000**, *174*, 375.

6 B. M. Razavizadeh, S. M. Mousavi-Khoshdel, H. Gharibi, R. Behjatmanesh-Ardakani, B. Sohrabi, S. Javadian, *J. Colloid Interface Sci.* **2004**, *276*, 197.

7 M. Sjöberg, R. Silveston, B. Kronberg, *Langmuir* **1993**, *9*, 973.

8 I. Szlifer, A. Ben-Shaul, W. M. Gelbart, *J. Chem. Phys.* **1985**, *83*, 3597.

9 R. Nagarajan, E. Ruckenstein, *J. Colloid Interface Sci.* **1983**, *91*, 500.

10 R. G. Larson, *Curr. Opin. Colloid Interface Sci.* **1997**, *2*, 361.

11 R. G. Larson, *J. Chem. Phys.* **1988**, *89*, 1642.

12 S. Karaborni, K. Esselink, P. A. J. Hilbers, B. Smit, J. Karthäuser, N. M. van Os, R. Zana, *Science* **1994**, *266*, 254.

13 A. Bhattacharya, S. D. Mahanti, A. Chakrabarti, *J. Chem. Phys.* **1998**, *108*, 10281.

14 H. E. Alper, T. R. Stouch, *J. Phys. Chem.* **1995**, *99*, 5724.

15 C. M. Wijmans, P. Linse, *Langmuir* **1995**, *11*, 3748.

16 P. Adriani, Y. Wang, W. L. Mattice, *J. Chem. Phys.* **1994**, *100*, 7718.

17 F. K. von Gottberg, K. A. Smith, T. A. Hatton, *J. Chem. Phys.* **1997**, *106*, 9850.

18 L. A. Rodriguez-Guadarrama, S. K. Talsania, K. K. Mohanty, R. Rajagopalan, *Langmuir* **1999**, *15*, 437.

19 J.-C. Desplat, C. M. Care, *Mol. Phys.* **1996**, *87*, 441.

20 C. M. Care, T. Dalby, J.-C. Desplat, *Prog. Colloid Polym. Sci.* **1997**, *103*, 130.

21 D. Stauffer, N. Jan, Y. He, R. B. Pandey, D. G. Marangoni, T. Smith-Palmer, *J. Chem. Phys.* **1994**, *100*, 6934.

22 A. Bhattacharya, S. D. Mahanti, *J. Phys.: Condens. Matter* **2000**, *12*, 6141.

23 M. Girardi, W. Figueiredo, *J. Chem. Phys.* **2000**, *112*, 4833.

24 S. K. Talsania, Y. Wang, R. Rajagopalan, K. K. Mohanty, *J. Colloid Interface Sci.* **1997**, *190*, 92.

25 A. T. Bernardes, V. B. Henriques, P. M. Bisch, *J. Chem. Phys.* **1994**, *101*, 645.

26 C. M. Care, T. Dalby, *Europhys. Lett.* **1999**, *45*, 38.

27 S. K. Talsania, L. A. Rodriguez-Guadarrama, K. K. Mohanty, R. Rajagopalan, *Langmuir* **1998**, *14*, 2684.

28 H. Gharibi, M. Hashemianzadeh, B. M. Razavizadeh, *Colloids Surf., A* **2002**, *196*, 31.

29 P. H. Nelson, G. C. Rutledge, T. A. Hatton, *J. Chem. Phys.* **1997**, *107*, 10777.

30 P. H. Nelson, Ph. D. Thesis, Massachusetts Institute of Technology, U.S.A., **1998**.

31 S. W. Haan, R. Pratt, *Chem. Phys. Lett.* **1981**, *79*, 436.

32 R. G. Larson, L. R. Scriven, H. T. Davis, *J. Chem. Phys.* **1985**, *83*, 2411.

33 R. G. Larson, *J. Chem. Phys.* **1989**, *91*, 2479.

34 R. G. Larson, *J. Chem. Phys.* **1992**, *96*, 7904.

35 R. G. Larson, *Chem. Eng. Sci.* **1994**, *49*, 2833.

36 R. G. Larson, *J. Phys. II* **1996**, *6*, 1441.

37 A. D. Mackie, K. Onur, A. Z. Panagiotopoulos, *J. Chem. Phys.* **1996**, *104*, 3718.

38 M. A. Floriano, E. Caponetti, A. Z. Panagiotopoulos, *Langmuir* **1999**, *15*, 3143.

39 S.-Y. Kim, A. Z. Panagiotopoulos, M. A. Floriano, *Mol. Phys.* **2002**, *100*, 2213.

40 A. Z. Panagiotopoulos, M. A. Floriano, S. K. Kumar, *Langmuir* **2002**, *18*, 2940.

41 M. T. Gurler, C. C. Crab, D. M. Dahlin, J. Kovac, *Macromolecules* **1983**, *16*, 398.

42 P. H. Verdier, W. H. Stockmayer, *J. Chem. Phys.* **1962**, *36*, 227.

43 P. De Gennes, *J. Chem. Phys.* **1971**, *55*, 572.

44 F. T. Wall, F. Mandel, *J. Chem. Phys.* **1975**, *63*, 4592.

45 M. Murat, T. A. Witten, *Macromolecules* **1990**, *23*, 263.

46 J. Reiter, T. Edling, T. Pakula, *J. Chem. Phys.* **1990**, *93*, 837.

47 J. I. Siepmann, D. Frenkel, *Mol. Phys.* **1992**, *75*, 59.

48 N. Metropolis, A. W. Rosenbluth, M. N. Rosenbluth, A. H. Teller, E. Teller, *J. Chem. Phys.* **1953**, *21*, 1087.

49 N. Madras, A. D. Sokal, *J. Stat. Phys.* **1987**, *47*, 573.

50 Z. A. Al-Anber, J. B. i Avalos, M. A. Floriano, A. D. Mackie, *J. Chem. Phys.* **2003**, *118*, 3816.

51 A. D. Mackie, A. Z. Panagiotopoulos, I. Szlifer, *Langmuir* **1997**, *13*, 5022.

52 H. Gharibi, B. M. Razavizadeh, A. Rafati, *Colloids Surf., A* **1998**, *136*, 123.

53 M. Lisal, C. K. Hall, K. E. Gubbins, A. Z. Panagiotopoulos, *J. Chem. Phys.* **2002**, *116*, 1171.

54 J. N. Israelachvili, D. J. Mitchell, B. W. Ninham, *J. Chem. Soc., Faraday Trans. 2* **1976**, *72*, 1525.

55 Y. Wang, W. L. Mattice, D. H. Napper, *Langmuir* **1993**, *9*, 66.

56 M. Zaldivar, R. G. Larson, *Langmuir* **2003**, *19*, 10434.

57 C. Tanford, *The Hydrophobic Effect: Formation of Micelle and Biological Membrane*, Krieger, Malabar, FL, **1991**.

58 E. Ruckenstein, R. Nagarajan, *J. Phys. Chem.* **1975**, *79*, 2622.

59 A. Ben-Naim, F. H. Stillinger, *J. Phys. Chem.* **1980**, *84*, 2872.

60 A. D. Mackie, A. Z. Panagiotopoulos, S. K. Kumar, *J. Chem. Phys.* **1995**, *102*, 1014.

61 M. Girardi, W. Figueiredo, *Phys. Rev. E* **2000**, *62*, 8344.

62 C. B. E. Guerin, I. Szleifer, *Langmuir* **1999**, *15*, 7901.

63 R. E. Goldstein, *J. Chem. Phys.* **1986**, *84*, 3367.

64 C. M. Care, *J. Chem. Soc., Faraday Trans.* **1987**, *83*, 2905.

65 R. Behjatmanesh-Ardakani, *J. Chem. Phys.* **2005**, *122*, 204903.